

Photoinduced Electron Injection from Ru(dcbpy)₂(NCS)₂ to SnO₂ and TiO₂ Nanocrystalline Films

Gábor Benkő, Pasi Myllyperkiö,[†] Jie Pan,[‡] Arkady P. Yartsev, and Villy Sundström*

Department of Chemical Physics, Lund University, Box 124, S-22100 Lund, Sweden

Received October 21, 2002; E-mail: villy.sundstrom@chemphys.lu.se

Studying the ultrafast electron transfer (ET) from the photoexcited transition-metal complex Ru(dcbpy)₂(NCS)₂ [dcbpy = (4,4'-dicarboxy-2,2'-bipyridine)] (i.e., RuN3) to TiO₂ nanoparticles is of great fundamental significance.^{1–3} In addition, the RuN3-sensitized nanocrystalline TiO₂ film (RuN3–TiO₂) is at the heart of the Grätzel-type solar cell,¹ which, based on these two materials, yields an overall light-to-electricity conversion efficiency of about 7–10%.¹ In comparison, dye-sensitized solar cells based on RuN3-sensitized SnO₂ films (RuN3–SnO₂) show low conversion efficiencies.⁴ Could it be that the lower performance of the RuN3–SnO₂-based solar cells is caused by lower rate and yield of electron injection from the photoexcited state of RuN3 into the conduction band of SnO₂?—as the conduction band energetics of TiO₂ and SnO₂ are different.⁵ Recently, Asbury et al.⁵ and Bauer et al.⁶ reported that the electron injection in RuN3–SnO₂ occurs on the picosecond time scale in a nonexponential fashion, and it is considerably slower than for TiO₂. In the case of Bauer et al.,⁶ a substantial part of the measured signal had an unresolved (<200 fs) rise component, and it was not possible to conclude whether the ultrafast rise of the signal was due to excited state absorption or electron injection products.

Herein we report ultrafast transient absorption polarization measurements on RuN3-sensitized SnO₂ and TiO₂ nanocrystalline films (see Supporting Information for experimental details). The interpretation of the results is based on a model recently developed for RuN3–TiO₂ by our group^{2,3} and shows that the pathways of electron injection in both systems, RuN3–TiO₂ and RuN3–SnO₂, are the same: the femtosecond part of interfacial ET between RuN3 and TiO₂, and SnO₂ films occurs from the initially excited singlet metal-to-ligand charge transfer excited state (¹MLCT), while the picosecond part proceeds from the thermalized triplet MLCT (³MLCT) excited state.

Figure 1 displays the transient absorption kinetics measured on RuN3-sensitized semiconductor films in acetonitrile at 850 nm, following 530 nm excitation with ~25 fs laser pulses in the ¹MLCT absorption band of the sensitizer. For clarity and better comparison, the data from Figure 1A together with the kinetics of RuN3 in ethanol solution (RuN3–EtOH, no ET is occurring) are normalized differently in Figure 1B. Depending on the delay time between the pump and probe pulses, the spectrally broad laser pulse centered at 850 nm probes both the excited state evolution of the RuN3 and the electron injection from the different excited states of RuN3 into the semiconductors. In details, the instantaneous formation of the ¹MLCT state is followed by its ultrafast decay on the sub-hundred femtoseconds time scale. Two competing processes cause this: the femtosecond part of electron injection and intersystem crossing (ISC) to the dye triplet state. The decay of the ¹MLCT signal is overlapping with the rise of oxidized RuN3 molecule (RuN3⁺), injected electrons in the conduction band of the semiconductor

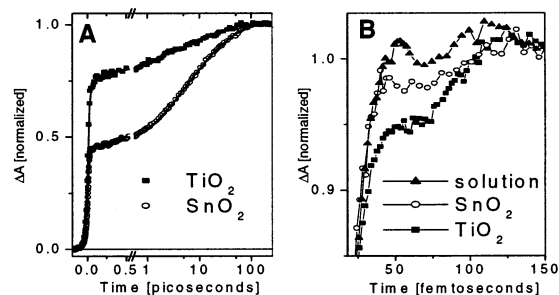


Figure 1. (A) Transient absorption kinetics measured on RuN3-sensitized TiO₂ and SnO₂ films in acetonitrile at 850 nm, normalized to the number of absorbed photons. Symbols are measured data, while curves are the best fits to the signals with the following time constants and amplitudes: TiO₂: rise within the laser pulse (73%), 1 ± 0.05 ps (13%), 10 ± 1 ps (8%), and 50 ± 5 ps (6%); SnO₂: rise within the laser pulse (44%), 2.5 ± 0.2 ps (18%), 10 ± 0.5 ps (22%), and 50 ± 1 ps (16%). (B) The same data as in panel A at early time, together with the kinetics measured on RuN3–EtOH at 850 nm, scaled at ~150 fs. The amplitude peak at ~50 fs delay time shows the decay of the ¹MLCT state. The extent ¹MLCT state is observed depends on the correlation between its lifetime and the instrument response function.

(e⁻TiO₂), and population of the triplet state. As a result, the ¹MLCT state is observed only as an amplitude peak with an indication of decay at ~75 fs delay time (Figure 1B). Finally, the triplet state is depopulated by electron injection on the picosecond time scale, resulting in the formation of RuN3⁺ and e⁻TiO₂ (>250 fs).^{2,3} For RuN3–EtOH the only channel for depopulation of the singlet state is ISC; hence, ET product is not formed. The quantum yield of the overall injection, given by the amplitude of the transient absorption kinetics of electron injection products at later delay times (>200 ps), is independent of the semiconductor (Figure 1A).

The time constants for the total singlet excited state deactivation of the two systems (RuN3–TiO₂ and RuN3–SnO₂) are resolved in this study when examining the time dependence of the absorption anisotropy of RuN3 (see Figure 2). For comparison, the rise of the anisotropy signal in RuN3–EtOH is also presented in the same figure. The time constants of 30 and 65 fs measured here for RuN3–TiO₂ and RuN3–EtOH, respectively, are in excellent agreement with previous measurements of singlet electron injection to TiO₂ (~30 fs) and ISC for RuN3 (~70 fs).^{2,3} For RuN3–SnO₂ singlet deactivation occurs with a time constant of ~45 fs. The obtained singlet deactivation rates for the different systems qualitatively agrees with the order in the decay of the singlet state (Figure 1B). Inserting the values of $k_{\text{TiO}_2} = 30$, $k_{\text{SnO}_2} = 45$, and $k_{\text{ISC}} = 65 \text{ fs}^{-1}$ in the rate equations for the two systems ($k_{\text{TiO}_2, \text{SnO}_2} = k_{\text{inj}} + k_{\text{ISC}}$), the rate of electron injection (k_{inj}) is estimated to be 1/55 and 1/145 fs⁻¹ for singlet ET in TiO₂ and SnO₂ films, respectively.

Previous^{2,3} and present results show that, the deactivation of the optically excited singlet state can be monitored in a number of ways, stimulated emission decay, photoproduct formation, triplet state

[†] Department of Chemistry, University of Jyväskylä, Finland.

[‡] Institute of Physics, Chinese Academy of Sciences, Beijing, China.

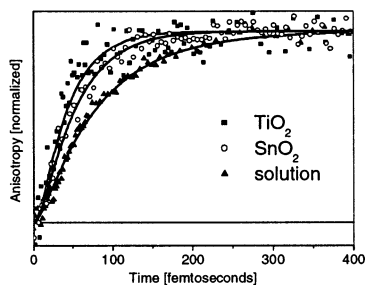


Figure 2. Time dependence of the scaled absorption anisotropy of RuN3–TiO₂, RuN3–SnO₂, and RuN3–EtOH. Symbols are measured data, while curves are fits to the signals with the following time constants: TiO₂ 30 ± 10 fs; SnO₂ 45 ± 5 fs; and EtOH 65 ± 10 fs. The measured changes in the amplitudes of the anisotropy signals on the presented time scale are ~0.02 for TiO₂ and SnO₂, and ~0.1 for EtOH.

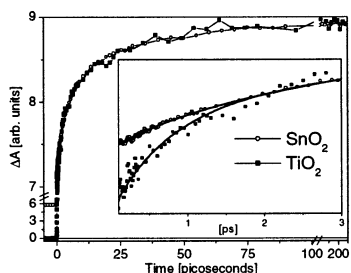


Figure 3. Triplet electron injection kinetics (induced rise of RuN3⁺ on the picosecond time scale) in RuN3-sensitized SnO₂ and TiO₂ films in acetonitrile at 850 nm, scaled on the >2 ps time scale. Inset: the same data between 0.1 and 3 ps. Symbols are measured data, while curves are fits to the signals with the following time constants and amplitudes: SnO₂ 2.5 ± 0.2 ps (32%), 10 ± 0.5 ps (39%), 50 ± 1 ps (28%); TiO₂ 1 ± 0.05 ps (48%), 10 ± 1 ps (30%), 50 ± 5 ps (22%).

formation, and change of anisotropy, providing a complete characterization of the process. The anisotropy measurements give not only the kinetics of singlet state deactivation but also more detailed information about the interfacial ET, which it will be presented elsewhere.⁷

Even though the ground state absorption spectra and adsorption properties of RuN3 on SnO₂ film (see Supporting Information) suggest that the electronic coupling between the carboxylated ligands of RuN3 and the SnO₂ surface is not very different from that of TiO₂ (according to ref 5, somewhat stronger for TiO₂), the lower rate of singlet state electron injection observed on SnO₂ is likely to be the result of a lower density of acceptor states in SnO₂.^{5–8} On the other hand, on the basis of reaction driving force alone, one expects faster electron-injection rate in SnO₂, as the SnO₂ conduction band is approximately 0.4 V more positive than that of TiO₂.^{1,5–8} The obtained result, that is, slower injection in SnO₂, is not consistent with the *driving force*-prediction of the classical ET theory implemented on such dye-sensitized nanoparticles.^{5,8}

Because of the very fast and efficient ISC, ~30 and ~65% of RuN3 molecules on TiO₂ and SnO₂, respectively, undergo ISC. After relaxation in the triplet excited state they inject electrons into the semiconductor on the picosecond time scale. The kinetics of this slower phase of electron injection are nonexponential and are identical for SnO₂ and TiO₂ for times >2 ps (Figure 3). The nonexponential behavior of the electron injection kinetics is probably a result of the inhomogeneous distribution of dye–semiconductor

interactions.^{5,6,8} On the basis of density of states and electronic coupling, similarly to electron injection from the singlet excited state, triplet state electron injection is expected to be faster in RuN3–TiO₂ than in SnO₂. An indication of these effects can be seen in the kinetics of Figure 3 inset, which shows that the rise of RuN3⁺ on the <2 ps time scale is slightly faster for TiO₂. Again, the expected influence of driving force on the rate of electron injection from the triplet excited state contradicts the observed dynamics.

Considering that SnO₂ and TiO₂ have different conduction band energetics,^{1,5,6} it is remarkable that the electron injection from the RuN3 triplet state is largely independent of the two semiconductors. The origin of this result should be found in the internal processes within the RuN3 molecule. Indeed, our recent experiments⁷ suggest that after thermalization of the triplet state,^{2,3} the electron injection occurs in concert with interligand electron transfer⁹ (ILET) from one bipyridine ligand of RuN3 to another. A detailed study of the role of ILET in triplet state ET will be presented elsewhere.⁷

In conclusion, we have shown that ET from RuN3 to SnO₂ film not only occurs on the picosecond but also on the femtosecond time scale. The time constants and the overall quantum yield of electron injection are similar for both RuN3–semiconductor systems. The rate of singlet ET is faster in TiO₂, presumably because of the higher density of acceptor states and favorable electronic coupling with RuN3. The triplet electron injection is controlled by internal processes (such as ILET) within the RuN3. Thus, while singlet electron injection does depend, the major part of triplet electron injection does not depend on the semiconductor. On the practical side, even though triplet injection is dominant in RuN3–SnO₂ and because of this the overall electron injection on SnO₂ is slightly slower than that on TiO₂, almost all the excited RuN3 molecules inject electrons within ~150 ps to both semiconductors. As a result, the electron injection process is most likely not responsible for the poor performance of the solar cell based on RuN3–SnO₂, although additional measurements on functioning solar cells are needed to establish such speculations.

Acknowledgment. We thank Mr. Jani Kallioinen for helpful discussions and assistance with the experiments. This research was funded by grants from the Delegationen för Energiförsörjning i Sydsvetig (DESS) and the Swedish Science Research Council.

Supporting Information Available: Femtosecond spectrometer, RuN3-sensitized semiconductor thin films (PDF). This material is available free of charge via the Internet at <http://pubs.acs.org>.

References

- (1) Grätzel, M. *Nature* **2001**, *414*, 338.
- (2) Benkö, G.; Kallioinen, J.; Korppi-Tommola, J. E. I.; Yartsev, A. P.; Sundström, V. *J. Am. Chem. Soc.* **2002**, *124*, 489.
- (3) Kallioinen, J.; Benkö, G.; Sundström, V.; Korppi-Tommola, J. E. I.; Yartsev, A. P. *J. Phys. Chem. B* **2002**, *106*, 4396 and references therein.
- (4) Chappel, S.; Chen, S.-G.; Zaban, A. *Langmuir* **2002**, *18*, 3336.
- (5) Asbury, J. B.; Hao, E.; Wang, Y.; Ghosh, H. N.; Lian, T. *J. Phys. Chem. B* **2001**, *105*, 4545 and references therein.
- (6) Bauer, C.; Boschloo, G.; Mukhtar, E.; Hagfeldt, A. *Int. J. Photoenergy* **2002**, *4*, 17.
- (7) Benkö, G.; Kallioinen, J.; Myllyperkiö, P.; Korppi-Tommola, J. E. I.; Yartsev, A.; Sundström, V. Manuscript in preparation.
- (8) Tachibana, Y.; Rubtsov, I. V.; Montanari, I.; Yoshihara, K.; Klug, D. R.; Durrant, J. R. *J. Photochem. Photobiol., A* **2001**, *142*, 215.
- (9) Waterland, M. R.; Kelley, D. F. *J. Phys. Chem. B* **2001**, *105*, 4019.

JA029025J